Subscripts

i = i^{th} curve
o = reference drop volume
n = n^{th} moment
nr = n^{th} moment with respect to the reference drop volume
r = reference curve

Superscripts

$\sim$ = modified similarity variable

LITERATURE CITED

Acrivos, A., and T. S. Lo, "Deformation and Breakup of a Single Slender Drop in an Extensional Flow," *J. Fluid Mech.*, **86**, 641 (1978).

Allen, T., *Particle Size Measurement*, Chapman and Hall, Ltd, MacMillan, New York (1959).

Barthe's - Biesel, D., and A. Acrivos, "Deformation and Burst of a Liquid Droplet Freely Suspended in a Linear Shear Field," *J. Fluid Mech.*, **61**, 1 (1973).

Berg, R. H., "Electronic Size Analysis of Sub-Sieve Particles by Flowing Through a Small Liquid-Resistor," Symposium on Particle Size Measurement, Sixty-First Annual Meeting Papers ASTM Special Technical Publication No. 234, p. 245 (1966).

Fillipov, A. F., "On the Distribution of the Sizes of Particles Which Undergo Splitting," *Theory Prob. Applic.*, **6**, 275 (1961).

Hinch, E. J., and A. Acrivos, "Steady Long Slender Droplets in Two-Dimensional Straining Motion," *J. Fluid Mech.*, **91**, 401 (1979).

Levich, V. G., Physicochemical Hydrodynamics, Prentice-Hall, Englewood Cliffs, N.J. (1972).

Madden, A. J., and B. J. McCoy, "Drop Size in Stirred Liquid-Liquid System Via Encapsulation," *Chem. Eng. Sci.*, **24**, 416 (1969).

Mlynek, Y., and W. Resnick, "Drop Sizes in an Agitated Liquid-Liquid System," *AIChE J.*, **18** 122 (1972).

Narsimhan, G., "Drop Breakage in Agitated Lean Liquid-Liquid Dispersions," Ph.D. dissertation, I. I. T. Kanpur, India (1979).

———, J. P. Gupta and D. Ramkrishna, "A Model for Transitional Breakage Probability of Droplets in Agitated Lean Liquid-Liquid Dispersions," *Chem. Eng. Sci.*, **34**, 257 (1979).

Ramkrishna, D., "On Problem Specific Polynomials," *Chem. Eng. Sci.*, **28**, 1362 (1973).

———, "Drop Breakage in Agitated Liquid-Liquid Dispersions," *ibid.*, **29**, 987 (1974).

Manuscript received October 1, 1979, and accepted January 23, 1980.

Photo-Assisted Heterogeneous Catalysis with Optical Fibers
II. Nonisothermal Single Fiber and Fiber Bundle

A previous paper (Marinangeli and Ollis, 1977) considered light transport in a single optical fiber which was coated with a heterogeneous photoassisted catalyst. This paper analyzes simultaneous mass, heat, and light transport in a catalyst on a single fiber, and in a likely large-scale configuration, a bundle of parallel, catalyst-coated optical fibers. The dimensionless temperature rise is dominated by energy released by light absorption, with the heat of reaction contributing to a lesser degree.

R. E. MARINANGELI

and

D. F. OLLIS

Dept. of Chemical Engineering
Princeton University
Princeton, NJ 08544

SCOPE

Photo-assisted catalysts are known to effect alkane partial oxidation, photo-electrolysis of water, and degradation of halogenated hydrocarbons, among other reactions. The potential for large-scale development of heterogeneous photo-assisted catalysis may likely require, *inter alia*, a large surface area per reactor volume for the transport of light to the catalyst surface. Our previous paper (Marinangeli and Ollis, 1977) suggested that catalyst-coated, small diameter optical fibers might satisfy such a criterion. This paper considers simultaneous transport of light, heat and reactant in two heterogeneous, photo-assisted catalyst configurations: the single coated fiber, and the bundle of parallel coated fibers.

Literature reports of quantum yields (molecules converted per photon absorbed) are usually 0.1 to 10%, and typical photon energies are of the order of a moderate heat of reaction. Consequently, for single fibers or fiber bundles, the dimensionless temperature rise is necessarily dominated by energy released on light absorption for all values of the Prater number. The approximate temperature independence of photochemical kinetics (below the temperature of catalyst deactivation) allows consecutive determination of concentration and temperature profiles. For catalysts which are inactive above temperature T^*, the dominant contribution of absorptive heating (unchanged by reaction) allows determination of the maximum useful bundle diameter for a given illumination intensity, or maximum intensity for a given bundle diameter. Transport limitations may lead to kinetics dominated either by slow mass diffusion or by insufficient local illumination.

This analysis applies to systems such as catalytic films of chloroplasts or other intact photosynthetic systems, metal complexes, or semiconductors. The special case of semiconductors which function as photoelectrodes when coated on optical fibers is analyzed in a subsequent paper (Marinangeli and Ollis, 1980).

Correspondence concerning this paper should be addressed to D. F. Ollis, Dept. of Chemical Engineering, Univ. of California, Davis, CA 95616.

R. E. Marinangeli is presently with Universal Oil Products, Des Plaines, Ill.

0001-1541-80-1000-9626-$01.05.

CONCLUSIONS AND SIGNIFICANCE

Simultaneous heat, mass and light transport may be important during photo-assisted heterogeneous catalysis. The maximum dimensionless temperature rise includes a light absorption heating term of the form:

$$F = \frac{d_p^2 \alpha_c I_o \beta'_c \exp(-\phi\xi)}{k_e T_o},$$

***where* d_p is a light penetration length. The reactant concentration profile for the isothermal or temperature independent first-order reaction in a layer of photo-assisted catalyst coated onto an optical fiber is given by:**

$$a = c_1 I_o(ME^{-\gamma}) + c_2 K_o(Me^{-\gamma}),$$

where I_o and K_o are modified Bessel functions; M is a Thiele modulus; and γ is a radial length. The reactant concentration in a long bundle of catalyst-coated fibers in the absence of axial diffusion and with radial Thiele modulus N is:

$$\hat{a} = \frac{I_o(N\rho)}{I_o(N)}.$$

The corresponding effectiveness factors including light and mass transport influences suggest the proper intensity for optimum photon and catalyst use.

Heterogeneous, photo-assisted catalysts are substances which require photo-excited electrons or holes in the course of a heterogeneously catalyzed reaction. Examples include metal complexes such as chlorophyll in natural chloroplasts, and a number of semiconducting oxides such as TiO_2. Irradiated TiO_2 is active in selective oxidation of alkanes (Formenti et al., 1971, 1974). Carbon monoxide oxidation occurs over illuminated ZnO (Murphy et al., 1976). Polychlorinated biphenyls are reported to be dechlorinated by irradiated TiO_2 (Carey et al., 1976). Semiconductors can be used for the photo-assisted electrolysis of water (Wrighton et al., 1975; Wrighton et al., 1976a, 1976b, 1976c; Ellis et al. 1976; Nozik, 1976). The prospects for solar energy conversion are particularly interesting. Dye sensitization can extend the light absorption range of these catalysts well into the visible region (Fleischauer and Allen, 1977; Fujishima et al., 1976).

A conceptual problem for scale-up of such heterogeneous photo-assisted catalysts is the requirement for supply of light to a large surface area of catalyst. A previous paper (Marinangeli and Ollis, 1977) reviewed the various reported heterogeneous, photo-assisted catalysts and considered a novel scale-up configuration, potentially applicable to all such catalysts: the catalyst-coated optical fiber of Figure 1a. In this new configuration, light incident on the end of an optical fiber would be "piped" down the fiber and "leak" into the annular catalyst layer coating the fiber. The high light transfer area per unit volume may be obtained, since fiber diameters as small as 10μ are commercially available.

A consideration of light transport in such photo-assisted catalysts indicated that the catalyst thickness could vary from a monolayer to many times the wavelength of the light. In each case, heat transport in the fiber should be included for two reasons. First, with present quantum yields (reaction event per absorption event) of from 0.1 to 10% and with photon energies of the order of typical heats of reaction, heat generation may be severe locally. Second, some photo-assisted catalysts are known to be heat-sensitive. For example, TiO_2 catalysts exhibit a rate for alkane partial oxidation which drops sharply above 110°C (Formenti et al., 1974). Biological photosynthetic systems would be similarly temperature-sensitive.

Most of the photo-assisted catalytic reaction will occur near the fiber-catalyst interface where the light intensity is greatest. The reactants will be supplied from the bulk gas or liquid phase adjacent to the catalyst-reactant interface and must diffuse through the porous concentric catalyst layer to reach the most intensely illuminated catalyst surfaces. Thus, mass transport must be considered.

Since practical applications will probably require light supply to many fibers and since individual 10-100 μm fibers may be impractical to handle, the catalyst-coated fibers may be bundled (Figure 1b), yielding the fiber bundle configuration used in optical communications. For the larger diameter fiber bundle, interfiber radial mass and energy transport influences will be more important than intrafiber effects in the single fiber.

MACROSCOPIC BALANCES

Steady-state mass and energy balances for a thick layer of photo-assisted catalyst coated onto an optical fiber are given by

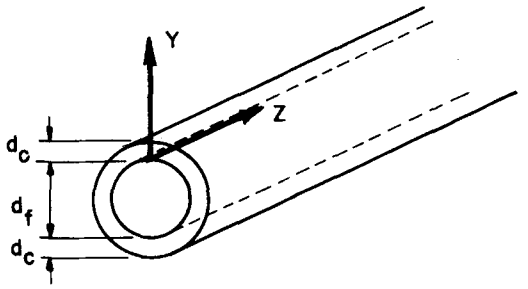

(a) COATED SINGLE FIBER

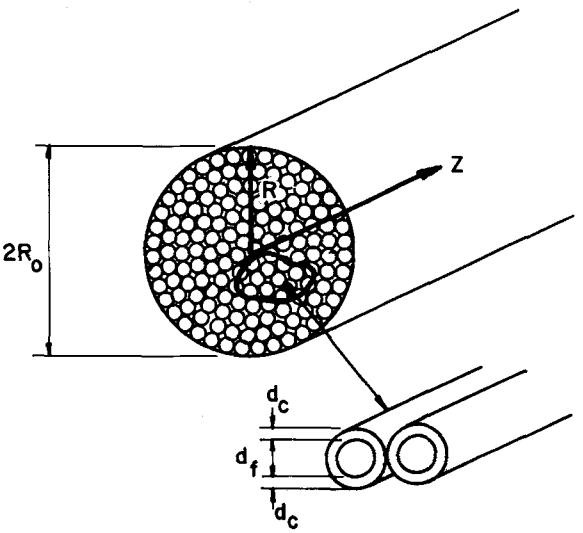

(b) FIBER BUNDLE

Figure 1. Schematic diagram of catalyst-coated optical fiber (a) and fiber bundle (b).

Eqs. 1 and 2, respectively.

$$D_e\left[\frac{\partial^2 A}{\partial y^2} + \frac{\partial^2 A}{\partial z^2}\right] + r\,(A,T,I) = 0 \qquad (1)$$

$$k_e\left[\frac{\partial^2 T}{\partial y^2} + \frac{\partial^2 T}{\partial z^2}\right] - (-\Delta H) r(A,T,I) + \alpha_c I_c = 0 \qquad (2)$$

The curvature of the concentric annular layer of photo-assisted catalyst is negligible (Marinangeli and Ollis, 1977). These equations for *monochromatic* light contain implicit wavelength dependencies in reaction rate, $r(A,T,I)$; intensity, I; and absorption coefficient, α_c. (The designation of the latter two terms as I and α is consistent with the literature of internal reflection spectroscopy, though different from convention in homogeneous photochemistry.)

Equations 1 and 2 are identical to the conservation equations for a conventional porous catalytic material except that: (i) the energy conservation equation contains a term for heat generation by de-excitations subsequent to light absorption and (ii) the reaction rate depends on intensity as well as concentration and temperature.

For a bundle of a large number of catalyst-coated optical fibers, the corresponding statements are:

$$\epsilon D_e\left(\frac{\partial^2 \hat{A}}{\partial R^2} + \frac{1}{R}\frac{\partial \hat{A}}{\partial R} + \frac{\partial^2 \hat{A}}{\partial z^2}\right) + \hat{r}(\hat{A},\hat{T},\hat{I}) f = 0 \qquad (3)$$

$$\epsilon K_e\left(\frac{\partial^2 \hat{T}}{\partial R^2} + \frac{1}{R}\frac{\partial \hat{T}}{\partial R} + \frac{\partial^2 \hat{T}}{\partial z^2}\right) - (-\Delta H)\hat{r}(\hat{A},\hat{T},\hat{I})\, f + \alpha_c \hat{I}_c f = 0 \qquad (4)$$

Here, averaged intrafiber quantities, designated by $\hat{}$, are used, since the bundle diameter is assumed much greater than that of a single fiber.

Nonisothermal Behavior

The mass and energy equations for a conventional heterogeneous catalyst each contain the reaction rate term which is a function of both temperature and concentration. Elimination of the reaction rate between the two equations allows direct integration to give the relationship between concentration and temperature at any point as a function of the boundary conditions (Damkohler, 1943; Prater, 1958). This result may be substituted into either the mass or the energy balance to give an equation containing only concentration or only temperature. From solution of the former, the nonisothermal effectiveness factor may be calculated (Weisz and Hicks, 1962).

For photo-assisted catalysts, the same procedure will be followed, but the results will contain a contribution due to absorption of illumination as seen from Eq. 2 or 4. Hence, an appropriate expression for the position dependent intensity within the catalyst must be determined. If the intensity in the catalyst is due only to the evanescent wave, the correct expression for a coated single fiber is (Marinangeli and Ollis, 1977):

$$I_c = \beta_c' I_o \exp\left(-\Phi\frac{z}{L} - 2\frac{y}{d_p}\right)$$

If the light is supplied to the catalyst only by scattering in the fiber or at the fiber-catalyst interface, a similar exponential intensity expression is obtained. The scattering contribution might dominate when the fiber diameter is very small or the particle size is of the order of the light wavelength (Marinangeli and Ollis, 1977). Unfortunately, the relative contributions from scattered and evanescent light cannot be easily determined. The case for contribution from both scattered and evanescent light can not be solved directly; a correct particular solution which is similar in form to the evanescent solution may be determined by trial and error in some cases. For simplicity, the expression for the evanescent wave only will be used throughout this paper.

The analysis is carried out in two steps. First, the single-fiber catalyst coating is analyzed; the integration is over the applied catalyst thickness, γ_c. Next, the bundle of optical fibers is considered.

The position-dependent average values of concentration ($\hat{A}$) and temperature ($\hat{T}$) in the bundle become boundary values for the individual fibers. The bundle contains many fibers. Thus, changes in $\hat{A}$ and $\hat{T}$ across the surface of a single fiber are negligible.

For a single fiber, eliminating the reaction rate from Eqs. 1 and 2 and rendering variables dimensionless yields Eq. 5 which relates temperature (θ) and concentration (a) for a layer of photo-assisted catalyst:

$$\frac{\partial^2}{\partial\gamma^2}(N_{Pr}a + \theta) + \frac{d_p^2}{L^2}\frac{\partial^2}{\partial\xi^2}(N_{Pr}a + \theta) + \mathrm{Fe}^{-2\gamma} = 0 \qquad (5)$$

The Prater number,

$$N_{Pr} = \frac{(-\Delta H) D_e A_o}{k_e T_o},$$

is the dimensionless ratio of maximum heat generation by chemical reaction to heat removal by conduction. The ratio of heat generation by light absorption to heat removal by conduction is given by:

$$F = \frac{d_p^2 \alpha_c I_o \beta_c' \exp(-\Phi\xi)}{k_e T_o}.$$

The conventional Prater number, N_{Pr}, does not contain an explicit length scale, since reactant and thermal energy are each transported by a diffusion term (second derivative). The light supply (for heat generation), however, falls off exponentially (first derivative). Thus, the dimensionless ratio, F, of light transport to heat transport by conduction must include a characteristic length of the system.

The second term in Eq. 5 may be neglected in the absence of large axial gradients, since $d_p << L$. With this assumption, the relation between concentration and temperature for the photo-assisted catalytic slab is found by integration to be:

$$(\theta - \hat{\theta}) = -N_{Pr}(a - \hat{a}) - \frac{1}{4}F(e^{-2\gamma} - e^{-2\gamma_c}) - \frac{1}{2}F(\gamma - \gamma_c) \qquad (6)$$

The boundary conditions are:

$$\frac{d\theta}{d\gamma}\Big|_o = \frac{da}{dy}\Big|_0 = 0,$$

$$\hat{a}(\gamma_c) = \hat{a},$$

and

$$\hat{\theta}(\gamma_c) = \hat{\theta}$$

For a single fiber,

$$\hat{a} = \hat{\theta} = 1.$$

In a fiber bundle, the concentrations and temperatures depend on the position within the bundle,

$$\hat{a} = \hat{a}(\rho,\xi),$$
$$\hat{\theta} = \hat{\theta}(\rho,\xi).$$

With conventional heterogeneous catalysts, the maximum dimensionless temperature rise equals the Prater number. Achievement of $(\theta - 1) = N_{Pr}$ occurs when $a = 0$ somewhere in the catalyst due to reaction. For heterogeneous photo-assisted catalysts, two limits on the dimensionless temperature rise may be noted. When ample illumination is provided, the reaction heating contribution is limited by mass diffusion. The maximum

dimensionless temperature rise occurs when $a = 0$ somewhere in the catalyst. When ample chemical reactant is provided, the dimensionless temperature rise is determined by light supply. The maximum dimensionless temperature rise occurs where the maximum amount of light is absorbed. The concentration does not equal zero in this case but falls to a value, a^*.

With a photo-assisted catalytic single fiber in the diffusion-limited regime ($a = 0$ at $\gamma = 0$), the maximum dimensionless temperature rise occurs at $\gamma = 0$:

$$(\theta - 1)_{max} = N_{Pr} + F\left(\frac{\gamma_c}{2} - \frac{1}{4}\right) \tag{7}$$

This expression has been simplified by noting that $e^{-2\gamma_c} \approx 0$ for thick catalyst layers, and by using $\hat{a} = \hat{\theta} = 1$. The dimensionless temperature rise equals the Prater number for reaction plus an additional dimensionless term due only to radiant absorptive heating.

For the light-limited case, the light absorption heating term remains the same. The reaction will not consume all of the reactant, though. The maximum dimensionless temperature rise occurs at $\gamma = 0$, again, where the concentration equals a^*, appreciably greater than zero. The smallest concentration gradient which could give $a = 0$ at $\gamma = 0$ is:

$$\left.\frac{dA}{dy}\right|_{y=d_c} \cong \frac{\hat{A} - A(0)}{d_c} \equiv \frac{A_o}{d_p}\frac{\hat{a}}{\gamma_c}$$

The total amount of light absorbed per unit fiber surface area is:

$$\int_o^{d_c} \alpha_c \beta_c' I_o \exp\left(-\Phi\frac{z}{L}\right)\exp\left(-2\frac{y}{d_p}\right)dy.$$

When this integral multiplied by the quantum efficiency is less than $D_e A_o \hat{a}/d_p\gamma_c$, the concentration does not equal 0 anywhere, hence the reaction heating term is less than the Prater number by a fraction which is the order of $(\hat{a} - a^*)$. Therefore,

$$(\theta - 1)_{max} \cong N_{Pr}(a - a^*) + F\left(\frac{\gamma_c}{2} - \frac{1}{4}\right), \tag{8}$$

and illumination-limited kinetics exist when

$$\frac{D_e A_o}{d_p}\frac{\hat{a}}{\gamma_c} > \int_o^{d_c} \chi\,\alpha_c\beta_c' I_o \exp\left(-\Phi\frac{z}{L} - \frac{-2y}{d_p}\right)dy$$

or

$$\frac{\hat{a}}{\gamma} > \frac{d_p^2 \chi \alpha_c \beta_c' I_o \exp(-\Phi\xi)}{2D_e A_o}.$$

The fraction $(\hat{a} - a^*)$ may be estimated by setting $da/d\gamma|_{\gamma_c} \cong (\hat{a} - a^*)/\gamma_c$,

$$\frac{\hat{a} - a^*}{\gamma_c} \cong \frac{d_p^2 \chi \alpha_c \beta_c' I_o \exp(-\Phi\xi)}{2D_e A_o}$$

or

$$\hat{a} - a^* \cong F \cdot \frac{\chi k_e T_o \gamma_c}{2D_e A_o} \tag{9}$$

Substitution of this expression into Eq. 8 gives:

$$(\theta - 1)_{max} \cong N_{Pr} F\left(\frac{\chi k_e T_o \gamma_c}{2D_e A_o}\right) + \frac{1}{2}F\left(\gamma_c - \frac{1}{2}\right)$$
$$= F\left[N_{Pr}\frac{\chi k_e T_o \gamma_c}{2D_e A_o} + \left(\frac{1}{2}\gamma_c - \frac{1}{4}\right)\right] \tag{10}$$

In the illumination-limited regime, the maximum dimensionless temperature rise is simply proportional to F, since the absorptive heating term and the light limited reaction rate are both proportional to F.

A similar analysis applies for the fiber bundle if axial diffusion is ignored ($L >> R_o$). Then,

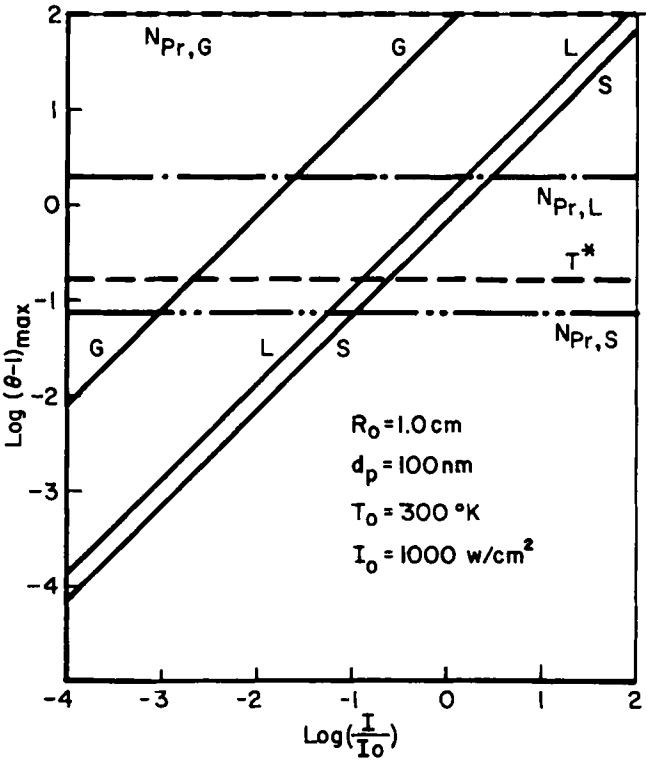

Figure 2. Log-log plots of maximum dimensionless temperature rise eqn (14), solid lines (T_o = 300°K) vs. dimensionless intensity ($I_o = 10^3$ W/m²).

Solid lines correspond to eqn (14) when typical gas (G), liquid (L) or solid (S) transport properties are assumed (see also Table 1) The temperature of catalyst deactivation is given by the dashed line (— — —), while the conventional Prater number is shown by the double broken line (—— — ——) for the porous solid, by the broken line (—— · ——) for the liquid, and by the small dashed line (----) for the gas.

$$\frac{1}{\rho}\frac{d}{d\rho}\left(\rho\frac{d}{d\rho}(N_{Pr}\hat{a} + \hat{\theta})\right) + \hat{F} = 0 \tag{11}$$

Here, $\hat{F}$ contains an averaging of intensity over individual fibers:

$$\bar{I}_c = \beta_c' I_o \exp(-\Phi\xi)\frac{\int_o^{\gamma_c} e^{-2\gamma}d\gamma}{\int_o^{\gamma_c} d\gamma}$$

$$= \frac{\beta_c' I_o \exp(-\Phi\xi)}{2\gamma_c}, \quad \text{when } e^{-2\gamma_c} \approx 0, \text{ and } d_c << d_f$$

(For thick catalyst films, with $d_c \approx \delta_f$, the intensity integral, $\int e^{-2\gamma}d\gamma$, may be taken over a slab volume, since the depth of penetration is still much less than the fiber thickness. The total volume, however, must be taken over a cylindrical cross-section, $\int 2\pi\gamma d\gamma$.

TABLE 1.

ΔH	$= 9.62 \times 10^5$ J/mol
D_e (gas)	$= 1 \times 10^{-5}$ m²/s
D_e (porous solid)	$= 1 \times 10^{-6}$ m²/s
D_e (liquid)	$= 1 \times 10^{-9}$ m²/s
A_o (liquid)	$= 5.5 \times 10^4$ mol/m³
A_o (gas)	$= 40$ mol/m³
T_o	= 300°K
d_f	$= 1 \times 10^{-4}$ m
d_c	$= 1 \times 10^{-6}$ m
k_e (gas)	$= 1.729 \times 10^{-2}$ J/m · s · °K
k_e (porous solid)	= 1.729 J/m · s · °K
k_c (liquid)	= 1. J/m · s · °K
α	$= 100$ m^{-1}
β	= 0.2
χ	= 0.1

$$\bar{I}_c = \frac{\beta_c' I_o \exp(-\Phi\xi)}{2\gamma_c + \frac{d_c}{2d_f}}, \quad \text{where } e^{-2\gamma_c} \approx 0, \text{ and } d_c \approx d_f$$

Using the result for averaging over a slab volume with $d_c \ll d_f$,

$$\hat{F} = \frac{R_o^2 \alpha_c I_o \beta_c' \exp(-\Phi\xi) f}{2k_e T_o \epsilon \gamma_c}$$

The relationship between concentration and temperature in the bundle is:

$$(\hat{\theta} - 1) = -N_{Pr}(\hat{a} - 1) - \hat{F}(\rho^2 - 1) \tag{12}$$

since $\hat{a}(1) = \hat{\theta}(1) = 1$. The maximum dimensionless temperature rise in the presence of sufficient light to give $a \simeq 0$ at $\gamma = 0$ is:

$$(\hat{\theta} - 1)_{\max} = N_{Pr} + \hat{F} \tag{13}$$

For the light-limited regime, N_{Pr} is diminished by the same factor of $(a - a^*)$ as in the single-fiber case, since light transport occurs only in the catalyst. This may be expressed as:

$$(\hat{\theta} - 1)_{\max} = N_{Pr}\left(F \frac{\chi k_e T_o \gamma_c}{2D_e A_o}\right) + \hat{F}$$

Since

$$F = \frac{2d_w^2 f}{\epsilon R_o^2} \hat{F},$$

the result may be written as:

$$(\hat{\theta} - 1)_{\max} = \hat{F}\left(1 + \frac{d_w^2 f \chi k_e T_o \gamma_c}{R_o^2 \epsilon D_e A_o}\right) \tag{14}$$

The ratio of d_p^2/R_o^2 indicates that the contribution due to reaction is small in comparison to the light absorption term.

Obviously, $\hat{F}$ can be larger than F since $R_o >> d_p$. In addition, the ratio of transport properties D_e/k_e will change depending on both the manner of assembling the bundle and the bulk reactant phase (gas or liquid). The Prater number will be larger for a loose bundle of coated fibers touching occasionally, separated by a gas phase, than for a tightly packed bundle with the transport properties of a porous solid. The upper limit for the Prater number is obtained with bundle transport properties equal to those of the gas phase. The Prater number is smallest for a bundle with porous solid thermal conductivity and effective diffusivity.

Calculated maximum dimensionless temperature rises for the fiber bundle are plotted in Figure 2 as a function of intensity which is dimensionless with respect to a peak solar flux. The parameters, which are shown in Table 1, are chosen for the isobutane partial oxidation reaction over illuminated TiO_2 (Formenti et al., 1971). These represent a typical quantum yield and heat of reaction. For this reaction, the maximum tolerable temperature rise is about 60°C ($\log(\theta - 1)_{\max} = -0.7$). Above this temperature the catalytic activity declines sharply. The energy flux of typical uv-lamps is on the order of 10^{-3} to 10^{-1} of the peak solar flux, which is 1 kW/m^2 (Bockris, 1975). Focussing systems can alter these values appreciably; e.g., nontracking solar concentrators can increase solar intensities by a factor of 10 (Rabl et al., 1974).

The dimensionless temperature rise is in the light-limited regime over most of the intensity range shown. At higher intensities, the reaction rate becomes diffusion limited; the contribution of the Prater number to the heat generation rate in this regime, however, is negligible in comparison to $\hat{F}$. Thus, the temperature rise over the entire range of intensities is dominated by $\hat{F}$.

The temperature rise for a single fiber is too low to be shown in Figure 2. The temperature rise for the bundle, however, is significant at moderate intensities. When gas-(porous solid) transport properties are used, the temperature increases into the catalyst deactivation region for intensities near the peak solar intensities. When gas-phase transport properties are used, the temperature rise is excessive even for moderate intensities. The result for liquid-phase properties is very similar to the porous solid result. Of course, for smaller bundles, the bundle temperature rise decreases as R_o^2.

In the presence of heat transfer resistance external to the bundle, the analyses of Lee and Luss (1969) and Carberry (1975) apply provided we replace N_{Pr} in their formulas by $(N_{Pr} + \hat{F})$ (diffusion limited case) or the equivalent expression for the light-limited case, Eq. 8 or 14. Thus, the total temperature rise ΔT within a fiber bundle is the sum of the internal and external contributions, given by:

$$(\theta - 1)_i = \frac{\Delta T_i}{T_o} = (N_{Pr} + \hat{F})(1 - \bar{\eta}Da)$$

and

$$\frac{\Delta T_{ex}}{T_o} = \frac{r'\bar{\eta}Da}{1 + \bar{\eta}Da\,(r - 1)}$$

where $\bar{\eta}Da$ is the observable global reaction rate divided by a calculable mass transfer rate and r' is the ratio of mass to thermal Biot numbers. While liquid-phase systems may be nearly isothermal, gas-solid systems will have a major portion of the overall ΔT external to the catalyst (Carberry, 1975). Hence, the total dimensionless ΔT of:

$$\frac{\Delta T_t}{T_o} = (N_{Pr} + \hat{F})(1 - \bar{\eta}Da) + \frac{r'\bar{\eta}Da}{1 + \bar{\eta}Da(r - 1)} \tag{15}$$

must be used to determine $(\theta - 1)_{\max}$. For exothermic photo-assisted reactions such as the catalyzed partial oxidation of alkanes considered here, a fiber bundle reactor may, therefore, require additional cooling (and/or smaller radius R_o) as the effect of $\hat{F}$, with present quantum efficiencies on the order of 0.1, is to increase the effective heat of reaction by a factor of 10 or more, without changing other properties of the porous gas-solid system.

When the temperature rise is excessive, an inactive catalyst core will be located at the interior of the catalyst near the fiber-catalyst interface. As the intensity is increased at the interface this core will grow, thereby reducing the active catalytic volume. At high enough intensities, the global reaction rate will decrease (as the entire catalyst approaches ≥80°C). Conversely, at low light intensities the reaction will be light limited. Obviously, an optimum light intensity range exists for obtaining the maximum global reaction rate.

Temperature-Independent First-Order Reaction

The preceding calculations have shown that an isothermal reaction could be assumed for many reactions for the single fiber, and for the fiber bundle, if the light intensity is modest.

In addition, the photo-assisted rate of alkane partial oxidation is reported to be independent of temperature between 50 and 80°C and increases only slightly between −15 and 50°C (Formenti et al., 1974). Hence, this system may be treated as temperature independent (analytically, appearing isothermal). When the rate expression, including the absorption coefficients and the diffusivity, is not strong functions of temperature, the concentration profile can therefore be determined independent of the temperature. The resulting concentration profile is used to calculate an effectiveness factor and a temperature profile for the temperature independent case.

Taking the isothermal or temperature independent rate expression as first order in both reactant A and intensity I,

$$r(A,I) = -k\chi\alpha_c I_c A$$

and the local intensity of the evanescent wave

$$I_c = \beta_c' I_o \exp\left(-\Phi \frac{Z}{L} - 2\frac{y}{d_p}\right)$$

the dimensionless mass conservation equation is

$$\frac{\partial^2 a}{\partial \gamma^2} + \frac{d_p^2}{L^2}\frac{\partial^2 a}{\partial \xi^2} - \frac{d_p^2 k \chi \alpha_c I_o \beta_c' \exp(-\Phi\xi - 2\gamma)}{D_e} \cdot a = 0 \quad (16)$$

Neglecting axial diffusion,

$$\left(\frac{\partial^2 a}{\partial \gamma^2} >> \frac{d_p^2}{L^2}\frac{\partial^2 a}{\partial \xi^2}\right)$$

yields the dimensionless mass conservation equation

$$\frac{d^2 a}{d\gamma^2} - M^2 e^{-2\gamma} a = 0 \quad (17)$$

The dimensionless group M is the local Thiele modulus for isothermal or temperature independent photo-assisted reactions:

$$M^2 = \frac{d_p^2 k \chi \alpha_c \beta_c' I_o \exp(-\Phi\xi)}{D_e}$$

Equations containing an exponential dependence of intensity (and hence reaction rate) on position are commonly obtained for homogeneous photochemical reactors. The average intensity is usually calculated and substituted into the equation to eliminate the γ dependence in the exponential (Huff and Walker, 1962; Cassano et al., 1967; Harano and Smith, 1968; Matsuura et al., 1969). An exact solution can be obtained for Eq. 17 with the following substitution:

$$u = Me^{-\gamma}$$

which yields a form of Bessel's equation,

$$u^2 \frac{d^2 a}{du^2} + u\frac{da}{du} - u^2 a = 0 \quad (18)$$

The concentration profile is given by:

$$a = c_1 \hat{I}_o(u) + c_2 \hat{K}_o(u) \quad (19)$$

where $\hat{I}_o$ and $\hat{K}_o$ are modified Bessel functions of the first and second kind, respectively. The constants may be evaluated from the boundary conditions,

$$a(\gamma_c, \xi) = \hat{a}$$

and

$$\frac{da}{d\gamma}(0,\xi) = 0$$

and the Bessel function properties,

$$\hat{I}_o'(x) = \hat{I}_1(x)$$

and

$$\hat{K}_o'(x) = -\hat{K}_1(x)$$

Thus,

$$c_1 = \hat{a}\left(\hat{I}_o(Me^{-\gamma_c}) + \frac{\hat{I}_1(M)}{\hat{K}_1(M)} \cdot \hat{K}_o(Me^{-\gamma_c})\right)^{-1}$$

and

$$c_2 = c_1 \frac{\hat{I}_1(M)}{\hat{K}_1(M)}$$

Of course, for a single isolated fiber $\hat{a} = 1$.

A radial effectiveness factor including light and mass transport influences in the thick, heterogeneous, photo-assisted catalytic film is, for a temperature-independent, first-order reaction:

$$\eta_r = \frac{\text{Actual reaction rate}}{\text{rate with no diffusional influences}}$$

$$= \frac{\text{surface}}{\text{volume}} \frac{D_e \left.\frac{dA}{dy}\right|_{d_c}}{k\alpha_c \chi \beta_c' I_o \exp(-\xi\Phi)}$$

$$= -\frac{1}{\gamma_c M^2} \cdot Me^{-\gamma_c} \left.\frac{da}{du}\right|_{u=Me^{-\gamma_c}}$$

$$= \frac{-e^{-\gamma_c}}{\gamma_c M}\left[c_1 \hat{I}_1(Me^{-\gamma_c}) - c_2 \hat{K}_1(Me^{-\gamma_c})\right]$$

For thick catalyst layers ($\gamma_c >> 1$), the radial effectiveness factor approaches $1/2\gamma_c$ (at $\xi = 0$). This unusual result is obtained because the average value of the evanescent light intensity is:

$$\bar{I}_c = \frac{\int_o^{\gamma_c} I_o e^{-2\gamma}\, d\gamma}{\int_o^{\gamma_c} d\gamma}$$

$$\bar{I}_c = I_o\left(\frac{1 - e^{-2\gamma_c}}{2\gamma_c}\right)$$

For $\gamma_c >> 1$, $\bar{I}_c$ equals $I_o/2\gamma_c$.

In the absence of mass transfer limitations, the effectiveness factor still cannot exceed $\bar{I}_c$. Of course, when $\gamma_c \to 0$, $\bar{I}_c/I_o$ approaches unity. The axially averaged radial effectiveness factor for the entire length of the coated optical fiber is:

$$\bar{\eta}(\rho) = \int_o^1 \eta_r(\rho,\xi) d\xi$$

Similarly, the reaction rate of the isothermal fiber bundle in terms of the bulk concentration is:

$$\hat{r}(\hat{A},\hat{I}) = -k_c \chi I_o \beta' \exp(-\Phi\xi)\hat{A}\,\eta_r(\xi)$$

Substitution of this expression into Eq. 3 yields:

$$\frac{\partial^2 \hat{a}}{\partial \rho^2} + \frac{1}{\rho}\frac{\partial \hat{a}}{\partial \rho} + \left(\frac{R_o}{L}\right)^2 \frac{\partial^2 \hat{a}}{\partial \xi^2} - N^2 \hat{a} = 0 \quad (20)$$

N is the Thiele modulus for the fiber bundle,

$$N^2 = \frac{R_o^2 k \alpha_c \chi \beta_c' I_o \eta_r(\xi) \exp(-\Phi\xi) f}{D_e \epsilon}$$

When axial diffusion is negligible, Eq. 20 is simply

$$\rho^2 \frac{d^2 \hat{a}}{d\rho^2} + \rho \frac{d\hat{a}}{d\rho} - \rho^2 N^2 \hat{a} = 0$$

with a solution of

$$\hat{a} = c_1 \hat{I}_o(N\rho) + c_2 \hat{K}_o(N\rho)$$

For boundary conditions $\hat{a}$ is finite and $\hat{a}(1,\xi) = 1$, the final expression for the concentration in the fiber bundle is:

$$\hat{a} = \hat{I}_o(N\rho)/\hat{I}_o(N)$$

An isothermal effectiveness factor for the effect of mass transport limitations in the fiber bundle is (see Appendix):

$$\eta_b = -\left.\frac{2}{\epsilon N^2}\frac{d\hat{a}}{d\rho}\right|_1 = \frac{2I_1(N\rho)}{\epsilon N I_o(N)}$$

Since $R_o >> d_p$, the bundle Thiele modulus, N, will be correspondingly larger than the single-fiber Thiele modulus, M. Except for large values of N, the value of M is sufficiently small that η_r equals its asymptotic value of $1/2\gamma_c$ for thick layers, or 1 for $\gamma_c \to 0$. The ratio of N to M is:

$$N/M = \frac{R_o}{d_p}\sqrt{\frac{f\eta_r}{\epsilon}}$$

It is interesting to compare the single-fiber effectiveness factor obtained here for an exponentially varying reaction rate to

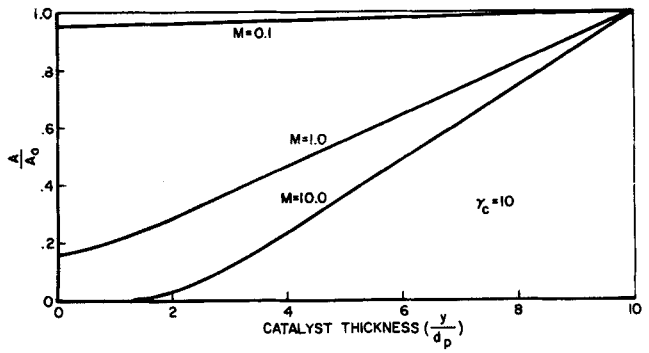

Figure 3. Dimensionless concentration in a single fiber plotted against the catalyst thickness for $\gamma_c = 10$.

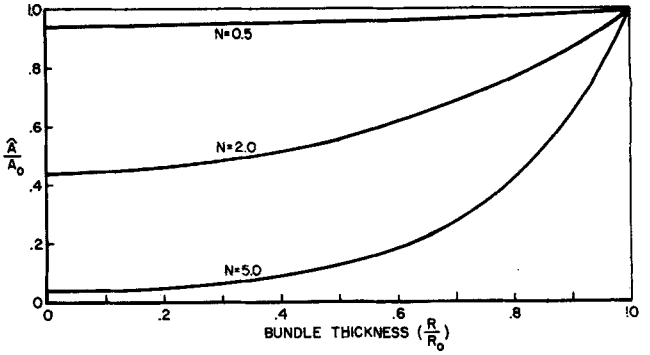

Figure 4. Dimensionless concentration in a fiber bundle plotted against the bundle radius.

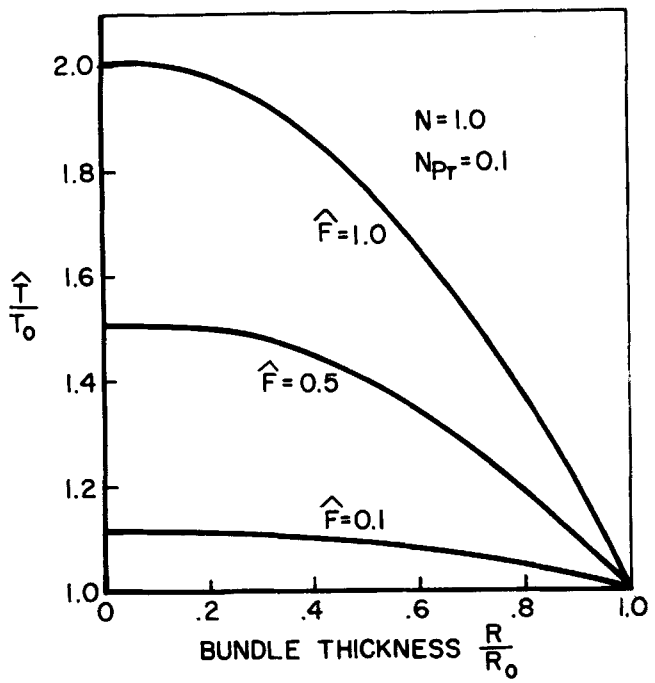

Figure 5. Dimensionless temperature rise in a fiber bundle. The concentration profiles are obtained from temperature independent kinetics with N = 1 for an exothermic reaction.

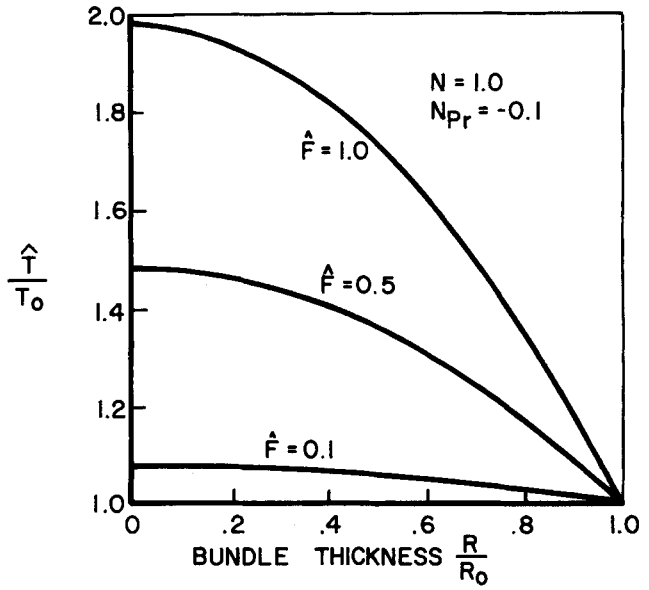

Figure 6. Dimensionless temperature rise in a fiber bundle. The concentration profiles are obtained from temperature independent kinetics with N = 1 for an endothermic reaction.

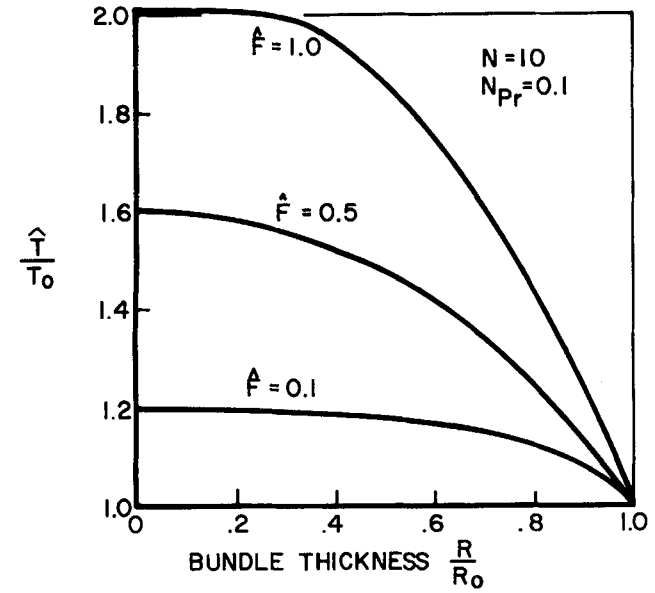

Figure 7. Dimensionless temperature rise in a fiber bundle. The concentration profiles are obtained from temperature independent kinetics with N = 10 for an exothermic reaction.

previous results for nonuniform catalytic activity. Effectiveness factors for linear or hyperbolic diffusivity or activity in a slab (Kasaoka and Sakata, 1968) and geometrically increasing activity for a sphere (Shadman-Yazdi and Peterson, 1972) both have an asymptotic limit equal to the inverse of the Thiele modulus for large values of the modulus. Indeed, it has been observed that the asymptotic behavior of the effectiveness factor is always the same for uniform or nonuniform activity, if, the Thiele modulus is based on the surface activity and the activity is nonzero at the surface.

Villadsen (1976) calculated the effectiveness factor for an isothermal pellet with activity decreasing towards the surface where the activity is zero. The form of the rate constant is $k = k_o(1 - x)^n$, *where* x is the dimensionless distance from the pellet center. The asymptotic value of the effectiveness factor equals the Thiele modulus to the $-(2n + 2)/(n + 2)$ power. For large n, the power approaches -2. This latter values is obtained if a shell of the pellet is completely poisoned (inactive) and acts as an external resistance. For any $n > 0$, the asymptotic value of the effectiveness factor never equals the limiting value of Thiele modulus to the -1 power.

At first, it would appear that our exponentially decreasing catalytic activity should give a result similar to the $k = k_o(1 - x)^n$ activity distribution. In fact, solutions for both cases are found by transforming to Bessel's equation. In our case, however, the effectiveness factor for the single fiber is proportional to the Thiele modulus to the -1 power. This corresponds to $n = 0$, or uniform activity in the Villadsen case. The reason that our asymptotic slope of log η vs. log M does not lie between -1 and

-2 is that the activity does not equal zero at the surface. It approaches zero for thick catalyst layers but never equals zero.

The concentration profiles for the single fiber and the fiber bundle are plotted in Figures 3 and 4, respectively, for several values of the appropriate Thiele modulus. The bundle profile is just the solution to the conventional (reaction & diffusion) equation for a "homogeneous" porous catalyst phase, $\nabla^2_\rho \hat{a} = k\hat{a}$ (k = constant), since the local averaging over a fiber yields $\eta_r(\xi)$ in the Thiele modulus (Eq. following Eq. 20).

For temperature-independent kinetics, the concentration profile may be substituted into the expression for the temperature profile. For the bundle, a concentration given by $\hat{a} = \hat{I}_o(N\rho)/\hat{I}_o(N)$ can be substituted into Eq. 12:

$$\hat{\theta} = 1 + N_{Pr}(1 - \hat{a}) + \hat{F}(1 - \rho^2)$$

From Figure 2, we recall that a typical Prater number for an exothermic reaction would be about 0.1 and a typical value for $\hat{F}$ would be about 0.1 to 1.0 at a solar intensity. The fiber bundle temperature profiles are shown in Figure 5 for these values of N_{Pr} and $\hat{F}$ with a Thiele modulus of 1. The effect of changing the Prater number to -0.1 (endothermic reaction) is shown in Figure 6. The effect of changing the Thiele modulus to 10 (steeper concentration gradient) is shown in Figure 7. The parabolic temperature profile for the bundle reflects the uniform heat generation within the bundle for each case, $\nabla^2_\rho \hat{T} = k(\xi)$.

APPENDIX

Fiber Bundle Effectiveness Factor

$$\eta = \frac{\text{surface}}{\text{volume}} \cdot \frac{D_e\left(\frac{dA}{dR}\right)\Big|_{R_o}}{k\chi\alpha_c I_o \beta' \exp(-\Phi\xi)\hat{A}\eta}$$

$$\frac{\text{surface}}{\text{volume}} = \frac{2\pi R_o L}{f\pi R_o^2 L} = \frac{2}{fR_o}$$

$$\eta = +\frac{2}{\epsilon}\frac{1}{N^2}\frac{da}{d\rho}\Big|_1 = \frac{2I_1(N)}{\epsilon N I_o(N)}$$

NOTATION

A = reactant concentration
A_o = A in region external to fiber bundle
$\hat{A}$ = A in fiber bundle
a = A/A_o in catalyst
$\hat{a}$ = $\hat{A}/A_o$ in fiber bundle
Da = Damköhler number
D_e = effective diffusivity
d_c = catalyst thickness
d_p = depth of penetration of evanescent wave
f = volume fraction of catalyst in fiber bundle
F = Heating number for light absorption in single fiber
$\hat{F}$ = Heating number for light absorption in fiber bundle
I = light intensity (taken equal to the energy flux density, energy per unit time per unit area)
I_c = light intensity in the catalyst
$\bar{I}_c$ = average intensity in the catalyst
I_o = initial light intensity in fiber
$\hat{I}_o(u)$ = modified Bessel function of the first kind
k = rate constant
k_e = effective thermal conductivity
$\hat{K}_o$ = modified Bessel function of the second kind
L = fiber length
M = Thiele modulus for single fiber
N = Thiele modulus for fiber bundle
N_{Pr} = Prater number, $(-\Delta H)D_e A_o/k_e T_o$
r = reaction rate
r' = ratio of mass to thermal Biot numbers
R = radial dimension of bundle
R_o = radius of fiber bundle
S_x = surface area of catalyst layer
T = temperature
ΔT_{ex} = temperature difference external to the catalyst
ΔT_i = temperature difference inside the catalyst
T_s = temperature at the exterior surface of the catalyst
T_o = temperature of region external to fiber bundle
T^* = temperature of catalyst deactivation
V_p = volume of catalyst layer
x = dimensionless distance from center of a catalyst pellet
y = radial distance in catalyst layer
z = axial distance

Greek Letters

α_c = absorption coefficient of catalyst
β'_c = ratio of light intensity in catalyst to intensity in fiber
γ = y/d_p
ϵ = void fraction in fiber bundle
η_b = effectiveness factor for the fiber bundle
η_r = effectiveness factor for the single fiber
θ = T/T_o
ξ = z/L
ρ = R/R_o
ϕ' or Φ = characteristic decay length for light in a fiber
χ = quantum efficiency
ψ = I/I_o

LITERATURE CITED

Bockris, J. O'M., *Energy: The Solar Hydrogen Alternative*, John Wiley and Sons, New York (1975).

Carberry, J. J., "On the Relative Importance of External-Internal Temperature Gradients in Heterogeneous Catalysis," *Ind. Eng. Chem. Fundam.*, **14**, 129 (1975).

Carey, J. H., J. Lawrence, and H. M. Tosine, "Photodechlorination of PCB's in the Presence of TiO_2 in Aqueous Suspensions," *Bull. Environ. Contam. Toxicol.*, **16**, 697 (1976).

Cassano, A. E., P. L. Silveston, and J. M. Smith, "Photochemical Reaction Engineering," *Ind. Eng. Chem.*, **59**, 18 (1967).

Corbett, W. E. Jr., and D. Luss, "The Influence of Non-Uniform Catalytic Activity on the Performance of a Single Spherical Pellet," *Chem. Engng. Sci.*, **29**, 1473 (1974).

Damköhler, G., "Excess Temperature in Catalyst Grains," *Z. Physik. Chem.*, **A193**, 16 (1943).

Ellis, A. B., S. W. Kaiser, and M. S. Wrighton, "Semiconducting Potassium Tantalate Electrodes: Photoassisted Agents for the Efficient Electrolysis of H_2O," *J. Phys. Chem.*, **80**, 1325 (1976).

Fleischauer, P. D., and J. K. Allen, "Photochemical Hydrogen Formation by Dye Sensitization of TiO_2 Thin Film Electrodes," *Aerospace Report* No. ATR-76 (8208)-1, The Aerospace Corp., El Segundo, CA.

Formenti, M., F. Juillet, P. Meriaudeau, and S. J. Teichner, "Heterogeneous Photocatalysis for Partial Oxidation of Paraffins," *Chem. Technol.*, **1** (1971).

Formenti, M., F. Juillet, and S. J. Teichner, "Systematic Study of the Heterogeneous Photocatalytic Oxidation of Hydrocarbons," Compte Rendu de Fin de Contrat d'une recherche financée par la Délégation générale à la recherche scientifique et technique, Contract No. 73 7 13 19 (1974).

Fujishima, A., T. Iwase, and K. Honda, "Effect of Irradiation with Ultraviolet Light on Spectral Sensitization of the Photoelectrochemical Process of a Zinc Oxide Single-Crystal Electrode," *J. Amer. Chem. Soc.*, **98**, 1625 (1976).

Harano, Y., and J. M. Smith, "Tubular Flow Reactors for Complex Nonchain Kinetics," *AIChE J.*, **14**, 584 (1968).

Huff, J. E., and C. A. Walker, "The Photochlorination of Chloroform in Continuous Flow systems," *AIChE J.*, **8**, 193 (1962).

Irazoqui, H. A., J. Cerda, and A. E. Cassano, "The Radiation Field for the Point and Line Source Approximations and the Three Dimen-

sional Source Models: Applications to Photoreactions," *The Chem. Eng. J.*, **11**, 27 (1976).
Kasaoka, S., and Y. Sakata, "Effectiveness Factors for Non-Uniform Catalyst Pellets," *J. Chem. Engng.*, Japan, **1**, 138 (1968).
Lee, J. C. M., and D. Luss, "Maximum Temperature Rise Inside Catalytic Pellets," *Ind. Eng. Chem. Fundam.*, **8**, 596 (1969).
Marinangeli, R. E., and D. F. Ollis, "Photoassisted Heterogeneous Catalysis with Optical Fibers: I. Isolated Single Fiber," *AIChE J.*, **23**, 415 (1977).
Marinangeli, R. E., and D. F. Ollis, "Photoassisted Heterogeneous Catalysis with Optical Fibers: III. Electron Transport for Photoassisted Electrolysis," In press (1980).
Matsurra, T., A. E. Cassano, and J. M. Smith, "AcetonePhotolysis: Kinetic Studies in a Flow Reactor," *AIChE J.*, **15**, 495 (1969).
Murphy, W. R., T. F. Verrkomp, and T. W. Leland, "Effect of Ultraviolet Radiation on Zinc Oxide Catalysts," *J. Catalysis*, **43**, 304 (1976).
Nozik, A. J., "Energy Conversion via Photoelectrolysis," *Proc. 11th Intersociety Energy Conversion Eng. Conf.*, **1**, 43 (Sept. 12-17, 1976).
Prater, C. D., "The Temperature Produced by Heat of Reaction in the Interior of Porous Particles," *Chem. Engng. Sci.*, **8**, 284 (1958).
Rabl, A., V. J. Sevcik, R. M. Giugler, and R. Winston, "Use of Compound Parabolic Concentrator for Solar Energy Use," Progress Report, Argonne National Lab, 75-42 (July-Dec., 1974).
Shadman-Yazdi, F., and E. E. Petersen, "Changing Catalyst Performance by Varying the Distribution of Active Catalyst within Porous Supports," *Chem. Engng. Sci.*, **27**, 227 (1972).
Villadsen, J., "The Effectiveness Factor for an Isothermal Pellet with Decreasing Activity towards the Pellet Surface," *Chem. Engng. Sci.*, **31**, 1212 (1976).
Weisz, P. B., and J. S. Hicks, "The Behavior of Porous Catalyst Particles in View of Internal Mass and Heat Diffusion Effects," *Chem. Engng. Sci.*, **17**, 265 (1962).
Wrighton, M.S., et al., "Photoassisted Electrolysis of Water by Irradiation of a Titanium Dioxide Electrode," *Proc. Nat. Acad. Sci.*, USA, **72**, 1518 (1975).
Wrighton, M. S., et al., "Photoassisted Electrolysis of Water by Ultraviolet Irradiation of an Antimony Doped Stannic Oxide Electrode," *J. Amer. Chem. Soc.*, **98**, 44 (1976a).
Wrighton, M. S., et al., "Strontium Titanate Photoelectrodes: Efficient Photoassisted Electrolysis of Water at Zero Applied Potential," *J. Amer. Chem. Soc.*, **98**, 2774 (1976b).
Wrighton, M. S., J. M. Bolts, A. B. Ellis, and S. W. Kaiser, "Photoassisted Electrolysis of Water: Conversion of Optical to Chemical Energy," *Proc. 11th Intersociety Energy Conversion Eng. Conf.*, **1**, 35 (Sept. 12-17, 1976c).

Manuscript received June 8, 1977; revision received April 28, and accepted May 5, 1980.

Hydrodynamic Effect of Surfactants on Gas-Liquid Oxygen Transfer

Y. H. LEE,
G. T. TSAO,
and
P. C. WANKAT

School of Chemical Engineering
Purdue University
West Lafayette, Ind. 47907

An experimental investigation of the hydrodynamics at the surface region of the liquid reveals that the soluble surfactants (sodium lauryl sulfate, glucose oxidase, and bovine serum albumin) affect both the length and the velocity scales of liquid eddies approaching the surface, which results in a decrease in mass transfer.

SCOPE

The effect of surfactant on gas-liquid mass transfer has been studied by numerous investigators due to its importance in industrial applications. For nonflow systems, surfactants were shown to exert considerable mass transfer resistances (Plevan and Quinn, 1966; Burnette and Himmelblau, 1970), whereas for flow systems such as falling films (Cullen and Davidson, 1956), stirred cells (Goodridge and Robb, 1965; Springer and Pigford, 1970), and channel flows (Moo-Young and Shoda, 1973), an additional effect, namely, the hydrodynamic effect was reported. This "hydrodynamic effect" means that the surfactant film at the surface of the liquid changes the interfacial hydrodynamics so that the mass transfer is reduced. Although it was shown theoretically (Davies, 1972) how the liquid eddy velocity is damped due to the surfactant, a detailed investigation of the "hydrodynamic effect" has been difficult mainly due to experimental limitations.

The objective of this study is to investigate the effect of some soluble surfactants on interfacial hydrodynamics for the oxygen absorption through a flat surface of a stirred cell. An oxygen ultra-microprobe was used for estimating the length and the velocity scales of liquid eddies approaching the surface.

CONCLUSIONS AND SIGNIFICANCE

The hydrodynamic effect was shown to be further broken down to two effects: an increase in the length scale and a decrease in the "equivalent" velocity scale of liquid eddies approaching the surface. The details of the hydrodynamic effect were different depending on the individual surfactant.

Correspondence for this paper should be sent to Y. H. Lee, who is presently with the Dept. of Chemical Engineering, Drexel University, Philadelphia, PA 19104.

0001-1541-80-4210-1008-$00.75.